Fabrication Techniques for Manufacturing Flexible Coils on Textiles for Inductive Power Transfer

Neil J. Grabham, Yi Li, Lindsay R. Clare, Bernard H. Stark, and Stephen P. Beeby, *Senior Member, IEEE*

Abstract— This paper presents a comprehensive evaluation of fabrication techniques for the integration of coils into textiles, for the purpose of enabling low-power wireless power transfer; for example, the powering of on-body monitoring devices, such as heart-rate monitors. Key electrical parameters of the coils required to maximize power transfer efficiency are identified from theory. Flexible coils have been fabricated using standard processes widely used in the textile industry, such as screen printing and embroidery. The screen printed coils were fabricated with a silver-polymer ink on a printed interface layer; the embroidered coils were fabricated using a variety of conductive threads formed by coating textile fibers and through the use of copper fibers. These coils have been experimentally characterized and evaluated for use in wireless power transfer applications. The effects of coil geometry and separation on the dc–dc power transfer efficiency using Qi standard compliant driver and receiver circuits are reported.

Index Terms— Flexible coils, inductive power transfer, smart textiles, wireless power transfer.

I. Introduction

INDUCTIVE power transfer (IPT) can be used to wirelessly transfer power over shorter distances of the order of centimetres to tens of centimetres. The basic mode of operation is that of an air-cored split transformer. A typical basic configuration consists of a transmitter coil energized by an external AC power source that causes an alternating magnetic field to be produced in the vicinity of the coil. When a second coil is bought into proximity of the magnetic field, energy is coupled from the transmitter coil to the receiver coil by their mutual inductance. The coils do not need to be in perfect alignment or in contact with one another, though increasing misalignment and separation will reduce the efficiency of power transfer. Inductive power transfer has found applications at a wide range of power transfer level requirements from transportation applications such as charging electric vehicles [1], the charging of consumer goods such as

mobile phones [2] to powering electronics embedded in the human body such as pacemakers [3].

This paper explores the use of inductive power transfer in textile based applications. The ability to integrate coils in textiles would enable body-worn systems mounted on, or integrated into the textile, to be powered or recharged wirelessly. Powering e-textile based autonomous systems is a considerable challenge and at present conventional rigid batteries are used. These have to be manually replaced when discharged and when garments are washed. Future e-textiles will be powered by integrated energy storage devices such as textile supercapacitors [4] and secondary batteries [5], but these will require recharging. Wireless IPT provides a convenient solution for recharging, but this requires the coil to be integrated into the textile in such a way that the properties and feel of the textile are unaffected.

Conductive coils can be realised on textiles using a number of fabrication processes familiar to the textile industry. Conductive tracks can be formed by weaving conducting wires into the textile as it is being manufactured. However, this constrains the direction of the conductive paths to that of the warp (along the length of the textile) and weft (across the width of the textile) and is not suitable for coil geometries. Other fabrication processes add the conductive tracks after the textile has been manufactured and can therefore be applied to any textile type. These processes include printing and stitching based techniques such as sewing, embroidery and overstitching conductive wire onto the surface of the textile. Textile coils fabricated using embroidered stainless steel yarns have previously been demonstrated, but the performance has not been compared with other fabrication techniques [6], [7]. IPT has also been demonstrated using a fabrication process that embeds conductors in silicone, resulting in a stretchable and flexible patch that can be subsequently attached to a textile [8]. This approach reduces the breathability of the textile and requires electrical connection to the textile after mounting the patch.

Each of these manufacturing processes, and the materials used, have implications for the properties of the coils and therefore the performance of the IPT. This paper explores these manufacturing processes for the fabrication of coils, and presents a theoretical and experimental evaluation of their effect on the IPT. The following section covers the basic IPT theory which is applied to theoretically evaluate the different coil properties on IPT performance. Section III introduces the manufacturing processes in more detail and presents an overview of their advantages and disadvantages. Sections IV

and V describe the manufacture of coils using the screen printing and stitching processes respectively, and presents the resulting coil properties. Section VI presents the theoretical evaluation of textile coil based IPT systems, and Section VII presents the corresponding experimental evaluations, which are compared in the discussion.

II. INDUCTIVE POWER TRANSFER

Ideally, when constructing coils for use in IPT applications, it is desirable to have low coil resistances to minimize resistive losses in the coils. This goal is more easily reached when using bulk materials such as copper wire. However, the manufacturing processes used to fabricate flexible coils on textiles can result in higher track resistances, resulting in coils with resistances which may have a significant effect on the efficiency and operation of the IPT system. Furthermore, the application and environment in which the coils are to be used may impose constraints on the dimensions of the coils. Many of the design constraints and objectives are interrelated, making the optimization of a textile coil design a non-trivial task, requiring compromises and trade-offs to be made.

The dependence of the power transfer efficiency, η_s, on the physical and electrical properties of the coils is shown in Equation 1 from Yates *et al.* [9],

$$\eta_s = \frac{\mu_0^2 \pi^2 N_{TX}^2 N_{RX}^2 \alpha_{TX}^4 \alpha_{RX}^4 \omega^2}{16 R_{TX} R_{RX} \left(\alpha_{TX}^2 + r^2\right)^3} \tag{1}$$

where μ_0 is the permeability of space, N_{TX} and N_{RX} are the number of turns in the transmitter and receiver coils respectively, α_{TX} and α_{RX} are the radii of the transmitter and receiver coils respectively, ω is the operating frequency, r is the separation between the coils and R_{TX} and R_{RX} are the resistances of the transmitter and receiver coils. This equation assumes a pair of coils axially aligned with the coils parallel and tuned to operate at the same frequency. From inspection we can see that for a pair of coils of given geometry, we wish to maximize the number of turns and minimize the coil resistances if we are to maximize the efficiency. In the equation, the coil resistances are given by

$$R_{TX} = R_{R_{TX}} + R_{L_{TX}} \tag{2}$$

$$R_{RX} = R_{R_{RX}} + R_{L_{RX}} \tag{3}$$

where R_R represents the radiation resistance and R_L the resistive losses in the coils. The resistive losses are attributable to the resistance of the conductive path forming the coil. The DC resistance of the conductive track for the transmitter coil is given by

$$R_{DC_{TX}} = \rho_{C_{TX}} \frac{l_{C_{TX}}}{w_{C_{TX}} t_{C_{TX}}} \tag{4}$$

where ρ is the resistivity of the conductor material and l, w and t are the length, width and thickness of the conductive track, respectively. Taking skin effect into account, the resistive losses for the transmitter coil are [10]

$$R_{L_{TX}} = R_{DC_{TX}} \frac{t_{C_{TX}}}{\delta_{TX} \left(1 - e^{-t_{C_{TX}}/\delta_{TX}}\right)} \tag{5}$$

where δ_{TX} is the skin depth in the TX coil and is given by

$$\delta_{TX} = \sqrt{\frac{2\rho_{C_{TX}}}{\mu_r \mu_0 \omega}} \tag{6}$$

where μ_0 is the permeability of space, μ_r is the relative permeability of the conductor and ω is the operating frequency. The resistive losses for the receiver coil can be found in the same manner.

By inspection of equations 1 to 6 it can be seen that the resistance of the coils is governed by the dimensions of the conductive track forming the coil windings, the number of turns and therefore the length of the conductor and also the operational frequency due to skin effect.

It can therefore be seen that the implementation of the coils involves a number of trade-offs in order to maximize the power transfer efficiency of the coil pair. For instance, increasing the number of turns in the coils will increase the efficiency (1), however this will also increase the length of the conductor which will increase its resistance if the cross sectional area remains the same, see (4). In fact, if the size of the coil is constrained, the width of the conductor may have to be reduced to accommodate the increased number of turns within the available space, further increasing the resistive losses. As a general rule it is desirable to minimize the resistance of the coil winding as far as possible within the design constraints, to permit a higher number of coil turns whilst still retaining an acceptable resistance to yield an acceptable overall efficiency.

Another key parameter affecting the coupling efficiency η_s between the two coils is their Q factor, and this is shown in Equation 7 [11]

$$\eta_s = \frac{k^2 Q_{TX} Q'_{RX}}{1 + k^2 Q_{TX} Q'_{RX}} \cdot \frac{Q_{RX}}{Q_{RX} + Q_L} \tag{7}$$

where Q_{TX} is the Q factor of the transmitter coil, Q_{RX} is the Q factor of the receiver coil, Q'_{RX} is the Q factor of the receiver coil under loading by the energy extraction circuitry, and Q_L is the Q factor of the receiver load network. k is the coils' coupling coefficient which is defined as

$$k = \frac{M}{\sqrt{L_{TX} L_{RX}}} \tag{8}$$

where M is the mutual inductance of the coils, and L_{TX} and L_{RX} are the inductances of the transmitter and receiver coils respectively. An approximate expression for k, in terms of the coil dimensions, is given by Equation 9 [12],

$$k \approx \frac{\alpha_{TX}^2 \alpha_{RX}^2}{\sqrt{\alpha_{TX} \alpha_{RX}} \left(\sqrt{r^2 + \max{(\alpha_{TX}, \alpha_{RX})}^2}^3\right)} \tag{9}$$

From these equations it can be seen that to maximize the transfer efficiency, the Q factors of the transmission and loaded receiver coil should be as high as possible. This can be achieved for a given drive frequency by maximizing the inductance of the coil whilst minimizing its resistance.

To illustrate these factors, theoretical example coils with a diameter of 100 mm, coil separation of 10 mm and unloaded Q factor of 10 will be analysed. The effect of increasing the

resistance of the receiver coil can be shown from (1). Doubling the receiver coil resistance R_{RX} whilst keeping the other parameters constant, will halve the power transfer efficiency. The effect of reducing the Q factor of the receiver coil can be shown using Equation 10 [11].

$$\eta_{s_{max}} = \frac{k^2 Q_{TX} Q_{RX}}{(kQ_{TX} + 1)(kQ_{RX} + 1)} \qquad (10)$$

This gives the maximum achievable efficiency as a function of Q factors and coupling efficiency, assuming the Q factor of the receiver coil load is optimum. The coupling factor k is found from the geometry using the approximate expression given by (9). Using the example coil details described previously, the maximum achievable efficiency $\eta_{s_{max}}$ for a system with two identical coils is 0.824. However, if the Q factor of the receiver coil were to halve, the maximum achievable efficiency falls to 0.754, a drop of 8.5% from the previous maximum efficiency. If the Q factor of both coils were to halve, the maximum achievable efficiency then becomes 0.691, a fall of 16.1%.

However, the scenario is further complicated since the Q factor is in turn a function of coil resistance as shown by equation 11,

$$Q_L = \frac{\omega L_L}{R_L} \qquad (11)$$

where Q_L is the Q factor of the coil, ω is the frequency of operation, L_L is the coil's inductance and R_L is the equivalent series resistance of the coil at the test frequency. An increase in coil resistance has a further negative effect on performance through the reduced coil Q-factor. Finally, the coil's parasitic capacitance is given by

$$C_P = 1/\left(4\pi^2 \omega_{SR}^2 L_L\right) \qquad (12)$$

where ω_{SR} is the self-resonant frequency of the coil.

This overview of IPT theory highlights the importance of the coil properties on the overall efficiency and performance of the power transfer system. The constraints imposed by the processes involved in fabricating coils in textiles will potentially compromise the coil properties with an associated effect on IPT performance. This will be explored practically in the following sections.

III. FABRICATION PROCESSES FOR FLEXIBLE COILS ON TEXTILES

The following range of fabrication processes have been selected because they are widely used by the textile industry and therefore compatible with existing manufacturing techniques.

A. Screen Printing

This process uses a screen printing technique to deposit functional (e.g. conductive) materials onto the surface of the textile. A flexible interface layer must first be printed onto the textile and cured. This layer serves to reduce the surface texture of the fabric and provide a smooth surface to which subsequent layers will bond successfully [13].The conductive material is formed into a paste and printed through a patterned

Fig. 1. Sewn on insulated conductor (conductor diameter 0.52 mm, stitch pitch of 1 mm).

screen to give the desired coil geometry on the textile. The printed film is then dried and cured to produce a stable film. To reduce the coil resistance, the film thickness is built up using repeated print and cure cycles. Multilayer coils can be achieved by printing a dielectric layer to separate the conductive layers. The screen printing process is applicable to volume batch production, and automated printing equipment is widely available. Whilst the cost of the screens may seem prohibitive for small numbers of coils, in a volume production situation this tooling-cost is shared between many printed devices. The primary cost for the printed coils is the silver paste used to print the conductor, the amount used depends on the geometry of the printed coil and the number of layers printed. Exact printing parameters and materials used in this work are discussed in Section IV.

B. Sewing and Embroidery Processes

Sewing-based processes include sewing and embroidering of conductive threads or wires onto textiles and the sewing on, or couching, conductive wire onto the textile surface. Sewing processes use a series of stitches to construct textile products and are used, for example, to join or finish fabrics. Embroidery is a decorative process used to add designs or features to a textile. In order to maintain compatibility with standard textile manufacturing processes, only automated techniques (as opposed to hand sewing and embroidery techniques) are considered here. The Pfaff Creative 3.0 automated sewing and embroidery machine used in this study has two thread paths: needle and bobbin path. In principle, conductive threads can be used simultaneously in both paths, producing a double-sided pattern However, this was found to be not possible with the conductive threads investigated in this study. The processes examined and evaluated in this work are as follows:

Single-sided sewing with conductive thread: conductive thread is used, to produce a number of stitched tracks, each of which relies upon the conduction along the length of the conductive thread to produce a conductive path across the textile.

Sewing on of insulated conductor as part of the stitch: this uses an insulated conductive wire in the lower thread path. Conventional non-conductive thread is used in the needle path to attach the conductive wire to the underside of the textile as shown in Fig. 1.

Single-sided embroidery with conductive thread: conductive thread is used as one of the two threads in the embroidery process. Embroidery can produce wider conductive tracks than

TABLE I

FEATURES OF VARIOUS SEWING AND EMBROIDERY PROCESSES

Process	Maximises conductor cross section	Able to produce conductor crossovers	Compatible with bobbin-only thread	Can readily produce low resistance	Compatible with stranded, flexible conductor
Single sided sewing with conductive thread	✗	✗	✓	1	-
Sewing on of an insulated conductor as part of the stitch	✗	✓	✓	✓	✓
Single sided embroidery with conductive thread	✗	✗	✓	1	-

✓ Feature can be achieved with the process
✗ Feature cannot be achieved by the process
- Feature does not apply to that process
1 Dependent on the conductive thread used

with sewing but relies upon conduction between adjacent stitches.

The key features of the various sewing and embroidery techniques are compared in Table I.

IV. FLEXIBLE TEXTILE COIL FABRICATION

This section presents the designs and fabrication of the flexible textile coils using screen printing and sewing processes.

A. Printed Coil Design

A single-layer coil design is employed in order to minimize the number of printed layers and therefore the effect on the flexibility of the textile. A circular coil is used which yields a shorter overall length and lower coil resistance than that of the square spiral for a given number of turns. This will also yield a higher unloaded Q factor. The outer diameter of the coil was 138mm. The silver-loaded conductive paste used to print the coil contains polymer binding agents, and therefore when cures it does not possess the conductivity of the base metal. Simulations [14] of the unloaded Q factor have been used to compare different combinations of track width and number of turns, resulting in the choice here of printing a six-turn coil with an external diameter of 138 mm, a track width of 4.5 mm, with a track spacing of 2 mm.

The coil is printed on a 65/35 polyester/cotton using a DEK 248 semi-automatic screen printer. The screens used for both the interface and conductive layers are made from a stainless steel mesh with a 40 μm emulsion. The interface layer (Fabink-IF-UV4, Smart Fabric Inks Ltd) is UV cured after each print cycle using 60 second exposure in a 400 W UV light cabinet system with an intensity of 50 mW/cm^3. Six interface layers result in a sufficiently smooth surface for subsequent processing. The silver-loaded conductive material (Fabink-TC-AG4002, Smart Fabric Inks Ltd) is thermally cured using a
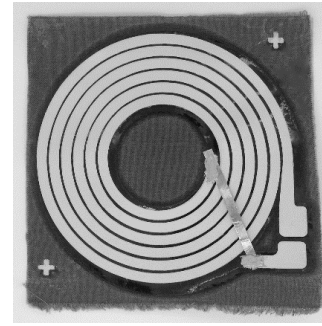

Fig. 2.   Printed coil, outer diameter 138 mm.

BTU DR92-5-60D belt dryer at a temperature of 130 °C for 40 minutes after each print cycle. Multiple print/cure cycles are used to achieve a nominal conductor thickness of 225 μm. A photo of the coil is shown in Fig. 2 and the full process details can be found in [14].

B. Sewn and Embroidered Coils

A range of conductive threads and wires have been evaluated with the sewing and embroidery processes discussed in Section III. Test tracks and coils were sewn and embroidered onto a standard Lagonda backing fabric (40% cotton, 30% elastane and 30% polyester). The choice of backing fabric has negligible effect on these processes. However, the coils themselves are more noticeable on finer backing fabrics.

1) Selection of Conductive Threads and Wires: The conductive threads typically consist of a core material, such as nylon, which is then coated with a conductive material such as silver. A range of core and conductive material combinations are commercially available and will be discussed below. In addition to the conductive threads, both solid core and stranded wires were investigated. Potential conductive materials were investigated for compatibility with the Pfaff Creative 3.0 automated sewing and embroidery machine. The key parameters that affect the suitability of the thread or wire for sewing and embroidery include:

- Diameter – the thread or wire must be a compatible in size with the needles used. Many of the readily available conductive threads are intended for the hobbyist market and are suitable for hand sewing but are too large for machine embroidery. Thread properties are given in Table II.
- Breaking strain – The thread or wire needs to be strong enough to withstand the tension applied during the sewing process, this requirement can rule out some of the thinner threads.
- Thread surface texture/roughness – The surface roughness affects how the thread or wire feeds through the embroidery machine. Excessive roughness increases the friction and can cause jams and snags in the machine.
- Abrasion resistance / fraying – if the thread or wire has a tendency to fray, it may bunch up and then jam in the needle, causing incomplete embroidery and/or thread breaks

The range of commercially available conductive threads and conductive wires evaluated in this study are summarised in Table II.

TABLE II
PROPERTIES OF CONDUCTIVE THREADS AND WIRES INVESTIGATED

	Material	DC Resistance Ω / m	Overall Diameter / mm	Insulation Working Voltage
Shieldex Statex 110/34 2-ply HC [15]	Silver on Nylon	< 100	0.068 mm	N/A
ARACON XS0200E-025 [16]	Silver on Kevlar	6.4	0.36 x 0.038 mm	N/A
Light Stitches conductive thread [17]	Silver on Nylon	40	0.22 mm	N/A
PTFE insulated flexible stranded 32 AWG wire [18]	Silver coated Copper	0.54	0.52 mm	250 V RMS
Litz wire silk covered 36/0.04 mm [19]	Enamelled Copper	0.55	0.30 mm	250 V RMS

TABLE III
COMPATIBILITY OF DIFFERENT THREADS AND WIRES WITH EACH PROCESS

Process	Shieldex Statex 110/34 2-ply HC	Aracon from Micro-Coax	Light Stitches conductive thread	Plain tinned solid core copper wire 35 SWG	PTFE insulated flexible stranded 32 AWG wire	Litz wire, silk covered 36/0.04 mm
Single sided sewing with conductive thread	✓	✗	✓	✗	✗	✗
Sewing on of an insulated conductor as part of the stitch	✗	✗	✗	✗	✓	✓
Single sided embroidery with conductive thread	✓	✗	✓	✗	✗	✗

The compatibility of these threads and wires was investigated by some initial sewing and embroidery tests. The compatibility with the various coil fabrication techniques is summarised in Table III.

For the test fabrication and material combinations shown in Table III, the following combinations were successfully fabricated:

- Shieldex "Statex" with single-sided embroidery and stitching.
- Conductive Thread from Light Stitches with single-sided embroidery and stitching.
- PTFE insulated flexible wire with stitching on of insulated conductor as part of the stitch.
- Silk covered Litz wire with stitching on of insulated conductor as part of the stitch.

The Micro-Coax "ARACON" is found to be abrasive, possibly due to its Kevlar base, with the ensuing friction and wear making it unsuitable for the embroidery machine used.
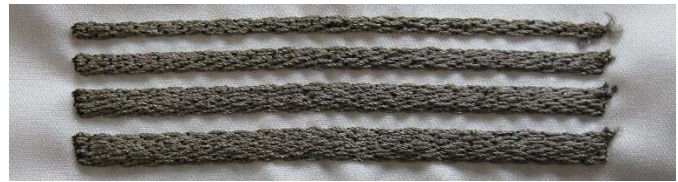

Fig. 3. Light Stitches single sided embroidered test tracks, widths 1 to 4 mm, 10 cm length.

TABLE IV
SINGLE SIDED EMBROIDERED LIGHT STITCHES
CONDUCTIVE THREAD TRACK RESISTANCES

Track Width	Track Resistance per m (stitch direction along length)	Track Resistance per m (stitch direction across width)
1 mm	18.7 Ω	44.3 Ω
2 mm	12.5 Ω	40.0 Ω
3 mm	7.5 Ω	32.9 Ω
4 mm	6.3 Ω	28.6 Ω

Whilst the Shieldex thread was found to be compatible with single sided sewing processes, it is not sufficiently conductive to realise coils with suitably low resistances. In summary, the upper needle thread path is found to be largely incompatible with the threads evaluated in this study, which means that the double-sided sewing and embroidery processes cannot be used to fabricate coils. Alternative automated sewing and embroidery machines may be compatible.

2) Track Resistance vs Stitch Direction: The embroidery process enables the conductive thread to be either stitched in the direction of the track or across the width of the track. The Light Stitches conductive thread was used to produce single-sided embroidered test tracks with widths of 1, 2, 3 and 4 mm. The embroidered 10 cm test tracks are shown in Fig. 3. Their measured DC resistances per m are shown in Table IV.

The Light Stitches test tracks shown in Fig. 3 shows the stiches aligned along the length of the track (left to right in the figure). The track resistance with the stitches aligned along the length of the track are less than half that of those aligned along the width. A typical coil design will require conductive tracks at more than one angle, with two directions being required for square coils and constantly varying direction being required for circular coils. To achieve the minimum resistance, the stitch direction must be changed depending upon the direction of the track. Whilst this is not possible for the embroidery process, the single-sided sewn track are formed by continuous stitching from one end of the track to the other, with the thread then stitched back again along the same path to build up the number of conductive threads between the ends of the conductive track. The track resistance achieved with this approach is 10 Ω/m using a total of four parallel threads with a width of 1.75 mm. This compares favourably with the resistances obtained using the embroidery process shown in Table IV and therefore the single-sided sewing approach using the Light Stitches conductive thread was used to produce test coils.

3) Test Coil Dimensions: The single-sided sewing process was used to fabricate both square and circular coils. The square coil is formed with 10 turns, an outer length of 87 mm, an inner length of 15 mm, and a pitch of 3.6 mm. The
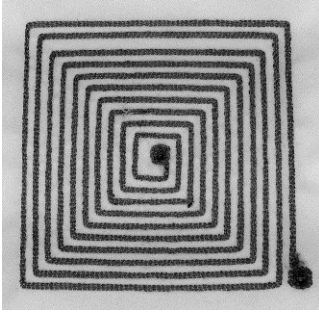
Fig. 4. Square-single sided sewn coils, Light Stitches conductive thread, outer diameter 87 mm.

Fig. 5. Circular sewn on coils, PTFE stranded wire, outer diameter 90 mm.

square coil has a track width of 1.69 mm and a DC resistance of 44 Ω (Fig. 4). A circular coil was also fabricated, this has 10 turns, outer diameter of 90 mm, inner diameter of 47 mm and a pitch of 2.5 mm. The track width is 1.70 mm and has a DC resistance of 120 Ω.

The sewn on coils with the PTFE coated stranded wires are fabricated to the same, 10-turn circular coil pattern as the single-sided sewn coil. This is shown in Fig. 5. The sewn on Litz wire is used to fabricate both the square and circular coils to the same dimensions as the sewn on PTFE coated wire coils.

V. FLEXIBLE TEXTILE COIL PROPERTIES

Basic electrical properties of the flexible coils were measured using a Wayne Kerr 6500B impedance analyzer over a frequency range from 10 kHz to 10 MHz to directly measure the inductance, and equivalent series resistance (ESR). The unloaded Q factors are calculated using (11) with the coils being operated at 1/10th of their self-resonant frequency and at 100 kHz and 200 kHz to cover the anticipated operating frequency range. A Rohde & Schwarz ZVB vector analyzer over a frequency range from 150 kHz to 100 MHz was used to measure the self-resonant frequency and this was used in conjunction with the coil inductance to calculate the parasitic capacitance using (12). The resulting properties are reported in Table V.

The Q-factor of the coils should be as high as possible in order to maximise the efficiency of the coil-to-coil power transfer. Both the screen-printed and single-sided sewn coils have Q-factors that are too low, and resistances that are too high to enable efficient wireless power transfer. In the case of the single-sided sewn coils the increased resistances introduce significant losses into the coils, resulting in the very low Q-factors. To reduce coil resistance, it would be necessary to use a conductive yarn with lower resistance and also a lower stitch-to-stich contact resistance. Other authors have addressed this issue by producing their own custom yarns, for example Heo *et al.* [20] used a silver filament twisted with polyester filaments to produce their yarn. Whilst the screen-printed coil has achieved a DC resistance comparable with that of the sewn on approach its Q-factor is lower and has a greater impact on the textile's feel and drape due to the printed track width and thickness. Reducing track dimensions without increasing coil resistance requires a more conductive ink and this may be developed in time. In contrast, the sewn on coils possess much better characteristics and provide also less obtrusive and more
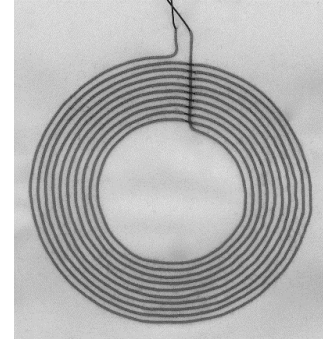
flexible solutions that have less of an effect on the feel of the textile. The circular spiral coils fabricated using sewn on PTFE insulated wire and the Litz wire have similar inductance and resistance values. The effect of the Litz wire construction is to increase the self-resonant frequency and therefore reduce the parasitic capacitance. The benefits associated with Litz wire relating to skin depth are not observed in these tests as the skin depth in a copper conductor at 1.08 MHz is 62 μm. The individual strands in the Litz (36-strand) and PTFE (7-strand) wires, are 40 μm and 79.9 μm in diameter respectively so in both cases the skin effect is not a significant concern. The construction of the Litz wire does, however, have the benefit of producing a compact and very flexible insulated conductor.

VI. POWER TRANSFER EFFICIENCY

The circular sewn on coils, made using PTFE insulated and Litz wire described in the previous section are tested for their overall power transfer efficiency. The end-to-end DC-DC transfer efficiency has been measured as this more accurately represents the overall system efficiency, as opposed to measuring the coil-to-coil efficiency as this does not take into account the losses in the driver and rectification circuitry. The losses and operational overhead in these stages are interrelated with the coil properties and as such should be treated as a whole system. In addition to the circular coils tested, a further Litz wire based, square coil is fabricated and tested; the result of this test is be discussed in Section VII.

The coils are tested using a commercially available Texas Instruments Qi standard compliant system, comprising a bq500211EVM evaluation driver system and a bq51013AEVM power receiver module, operating between 110 and 205 kHz. The coils are tuned to resonance at 100 kHz. The modules are supplied with rigid Litz wire wound power transfer coils; these coils are substituted with the flexible textile coils under test.

The measurement process used is as described by Li *et al.* [14], measurements of maximum power delivered to the load P_{output} and maximum DC-DC efficiency η_{DC-DC} are made at separations of 5, 10, 15 and 20 mm with the coils positioned so that they are aligned on-axis and with their substrates flat and parallel to one another. The results of these measurements are shown in Table VI. Also included in the table are theoretical maximum efficiencies for the coil pairs $\eta_{coil-Th}$, calculated using Equations 9 and 10, and theoretical system DC-DC efficiencies $\eta_{system-Th}$, calculated using a value

TABLE V
FLEXIBLE TEXTILE COIL PROPERTIES

Property	Screen Printed Coil	Single-sided Sewn Coil	Single-sided Sewn Coil [1]	Sewn on Coil (PTFE)	Sewn on Coil (Litz wire)	Sewn on Coil (Litz wire)
Geometry	Circular	Square	Circular	Circular	Circular	Square
Inductance (µH)	3.9	4.96	70.4	9.5	9.8	5.98
DC Resistance (Ω)	1.1	44	120	1.2	1.2	1.4
Equivalent Series Resistance at 1/10th of SRF (Ω)	12.0	48	-	3.5	75.1	46.1
Parasitic Capacitance (pF)	5.34	3.23	-	5.80	0.18	1.03
Self Resonant Frequency (MHz)	17.6	20.0	-	10.8	59.6	58.8
Unloaded Q Factor at 1/10th of SRF	8.48	1.37	-	16.09	4.19 [2]	4.55 [3]
Unloaded Q Factor at 100 kHz	1.52	0.07	0.36	4.64	5.03	3.40
Unloaded Q Factor at 200 kHz	3.08	0.15	0.73	9.36	10.16	6.84

[1] It was not possible to reliably establish the SRF of the circular single-sided sewn coil, therefore the figures dependant on this value cannot be reported.
[2] The unloaded Q factor for the circular Litz wire coil is lower than that of the PTFE wire due to its higher equivalent series resistance at the test frequency, measuring the Litz wire coil at the same frequency as the PTFE wire coil (1.08 MHz) gives an ESR of 3.7 Ω and a Q factor of 16.66.
[3] Measuring the square Litz wire coil at the operating frequency of the PTFE wire coil, 1.08 MHz, gives an ESR of 2.8 Ω and a Q factor of 14.58.

TABLE VI
MAXIMUM OUTPUT POWER AND EFFICIENCIES OF WIRELESS POWER TRANSFER SYSTEM DEPLOYED WITH CONDUCTIVE WIRE COILS

Separation	Symbol	Circular coils (PTFE)	Circular coils (Litz)	Square coils (Litz)
5 mm	P_{output}	2.06 W	2.05 W	2.15 W
	$\eta_{DC\text{-}DC}$	35.4 %	35.2 %	33.3 %
	$\eta_{coil\text{-}Th}$	66.9 %	68.8 %	58.5 %
	$\eta_{system\text{-}Th}$	48.2 %	49.6 %	42.1 %
10 mm	P_{output}	1.79 W	1.68 W	1.43 W
	$\eta_{DC\text{-}DC}$	33.3 %	32.0 %	23.0 %
	$\eta_{coil\text{-}Th}$	64.7 %	66.7 %	55.0 %
	$\eta_{system\text{-}Th}$	46.6 %	48.0 %	39.6 %
15 mm	P_{output}	1.35 W	1.16 W	0.15W
	$\eta_{DC\text{-}DC}$	24.1 %	22.6 %	2.0 %
	$\eta_{coil\text{-}Th}$	61.0 %	63.1 %	49.5 %
	$\eta_{system\text{-}Th}$	43.9 %	48.4 %	35.6 %
20 mm	P_{output}	0.81 W	0.80 W	0.11 W
	$\eta_{DC\text{-}DC}$	14.6 %	15.4 %	1.5 %
	$\eta_{coil\text{-}Th}$	56.1 %	58.4 %	42.6 %
	$\eta_{system\text{-}Th}$	40.4 %	42.0 %	30.7 %

of 72 % efficiency for the drive and rectification circuits within the evaluation system as determined from their datasheet [21].

Comparing the results for the circular coils, it can be seen that the maximum power that can be transferred is reasonably similar for a given coil separation for both wire types. Likewise, comparing the DC-DC efficiency figures show that the values are in close agreement. The similarity in the efficiency of the PTFE insulated and Litz wire coils shows that the advantages associated with the skin depth effects provided by the Litz wire do not make a significant contribution at the operational frequencies used (low 100s of kHz) in this application. Comparing the measured DC-DC efficiency values with the theoretical values shows that the measured efficiency reduces faster with increasing separation compared to the theoretical maximum efficiency value. Comparing the achieved and theoretical maximum system efficiency values for the square format coils shows a more marked difference in values.

VII. CIRCULAR VS SQUARE COILS

Square and circular coils made using Litz wire are compared. The square coil has an outside width of 90 mm which matches the diameter of the circular coils. Both the circular and square coil can fit within the same overall square area, but the square coil encompassing a larger area within its turns than the circular coil. Comparing the coil properties as shown in Table V, it can be seen that the square coil exhibits a lower inductance than the circular coil and a higher resistance and parasitic capacitance. Their resonant frequencies and unloaded Q factors are similar in value, although the Q factor of the square coil is lower than that of the circular coil when measured at 1.08 MHz.

From the results presented in Table VI it can be seen that for a 5 mm separation distance the square format coil delivers more power (~5 % more) than the circular format coil. However, for separations of 10 mm and greater, the circular coil achieves a higher maximum transferred power than the square coil. At separations of 15 and 20 mm, the maximum power transferred by the square coil configuration is just 13 % of that transferred by the circular coils. Comparing the overall DC-DC efficiency values, it can be observed that the efficiency is less at all separations for the square format coils, especially at separation distances of 15 and 20 mm.

From these measurements it is clear the circular format coils should be used in preference over the square format to maximize system efficiency and power transfer levels in the majority of cases. It should also be further noted that for these tests the square coils were positioned with the sides of the square coils in alignment; in many real-world cases this is unlikely to be the case and rotational misalignment will further reduce the efficiency and operation of the power transfer system, whereas rotational misalignment is not an issue with the circular design coils.

VIII. CONCLUSIONS

In this paper screen printing, sewing and embroidery processes have been evaluated as routes to producing flexible coils on textiles for use in wireless power transfer systems. Since one application of such coils is to integrate them into items such as clothing, there are a number of areas in addition to their electrical properties that need to be considered. These additional properties include: the flexibility of the finished

coil; safety of the user; potential skin sensitivities or allergies; and user comfort. Of the various approaches evaluated within this work, some can be discounted due to poor electrical performance, such as the embroidered conductive tracks whose resistance prevented them from working at all effectively. The screen printed coils require an impermeable interface layer to be deposited onto the fabric for the coils to be printed onto which affects the breathability of the textile. From the coils presented here, those made using either the PTFE insulated wire or the silk covered enamelled Litz wire using a sewing on technique to attach the insulated conductor to the textile, offer the properties required to realise comfortable and practical textile coils for wireless power transfer. Coils made with both of these materials have been found to have similar electrical properties and to produce an acceptably flexible textile coil. The coils fabricated using the Litz wire are potentially more acceptable to the user, as the wire used is thinner and therefore adds less bulk and stiffness to the underlying textile. However, if the Litz wire was deemed unacceptable for some reason, the PTFE insulated coils would be an acceptable substitute, resulting in a slightly less flexible coil.

Circular coils were found to transfer more energy for coil separations greater than 5 mm than square coils, and power transfer is not affected by rotational alignment. Output powers in the range of 0.81 to 2.06 W with DC-DC transfer efficiencies of 14.6 to 35.4 % were achieved over a range of separations of 5 to 20 mm for the circular sewn-on coils, the maximum output power is ultimately limited by the input power available from the drive circuit used. For comparison the textile coils developed by Heo *et al.* [20] achieved 24 mW with 46.2 % transfer efficiency when operating at 6.78 MHz with a 5 cm spacing, they also noted that their transfer efficiency fell off rapidly for separations greater than 15 cm.

In overall conclusion the best configuration taking into account fabrication and performance would be to use circular coils formed using sewn on Litz wire as these give the best combined flexibility and electrical performance.

REFERENCES

[1] C.-S. Wang, O. H. Stielau, and G. A. Covic, "Design considerations for a contactless electric vehicle battery charger," *IEEE Trans. Ind. Electron.*, vol. 52, no. 5, pp. 1308–1314, Oct. 2005.

[2] S. Y. R. Hui and W. W. C. Ho, "A new generation of universal contactless Battery Charging platform for portable consumer electronic equipment," *IEEE Trans. Power Electron.*, vol. 20, no. 3, pp. 620–627, May 2005.

[3] G. Wang, W. Liu, M. Sivaprakasam, and G. A. Kendir, "Design and analysis of an adaptive transcutaneous power telemetry for biomedical implants," *IEEE Trans. Circuits Syst. I, Reg. Papers*, vol. 52, no. 10, pp. 2109–2117, Oct. 2005.

[4] K. Jost *et al.*, "Carbon coated textiles for flexible energy storage," *Energy Environ. Sci.*, vol. 4, no. 12, pp. 5060–5067, 2011.

[5] Y.-H. Lee *et al.*, "Wearable textile battery rechargeable by solar energy," *Nano Lett.*, vol. 13, no. 11, pp. 5753–5761, Oct. 2013.

[6] M. Catrysse, R. Puers, C. Hertleer, L. Van Langenhove, H. van Egmondc, and D. Matthys, "Towards the integration of textile sensors in a wireless monitoring suit," *Sens. Actuators A, Phys.*, vol. 114, nos. 2–3, pp. 302–311, Jan. 2004.

[7] J.-S. Roh, Y.-S. Chi, J.-H. Lee, S. Nam, and T. J. Kang, "Characterization of embroidered inductors," *Smart Mater. Struct.*, vol. 19, no. 11, p. 115020, Sep. 2010.

[8] R. Carta *et al.*, "Design and implementation of advanced systems in a flexible-stretchable technology for biomedical applications," *Sens. Actuators A, Phys.*, vol. 156, no. 1, pp. 79–87, Nov. 2009.

[9] D. C. Yates, A. S. Holmes, and A. J. Burdett, "Optimal transmission frequency for ultralow-power short-range radio links," *IEEE Trans. Circuits Syst. I, Reg. Papers*, vol. 51, no. 7, pp. 1405–1413, Jul. 2004.

[10] U.-M. Jow and M. Ghovanloo, "Design and optimization of printed spiral coils for efficient transcutaneous inductive power transmission," *IEEE Trans. Biomed. Circuits Syst.*, vol. 1, no. 3, pp. 193–202, Sep. 2007.

[11] M. W. Baker and R. Sarpeshkar, "Feedback analysis and design of RF power links for low-power bionic systems," *IEEE Trans. Biomed. Circuits Syst.*, vol. 1, no. 1, pp. 28–38, Mar. 2007.

[12] W. Wu and Q. Fang, "Design and simulation of printed spiral coil used in wireless power transmission systems for implant medical devices," in *Proc. Annu. Int. Conf. IEEE Eng. Med. Biol. Soc.*, Sep. 2011, pp. 4018–4021.

[13] K. Yang, R. Torah, Y. Wei, S. Beeby, and J. Tudor, "Waterproof and durable screen printed silver conductive tracks on textiles," *Textile Res. J.*, vol. 83, no. 19, pp. 2023–2031, Nov. 2013.

[14] Y. Li, N. J. Grabham, R. N. Torah, J. Tudor, and S. P. Beeby, "Smart textile based flexible coils for wireless inductive power transmission," to be published.

[15] *Shieldex 110/34 2-Ply HC Technical Data Sheet*. Accessed: Jan. 2, 2018. [Online]. Available: www.shopvtechtextiles.com/assets/images/Shieldex110_34_dtex_2_ply_HC_Premium_Line%20(2).pdf

[16] *Aracon XS0200E-025 Datasheet*. Accessed: Jan. 2, 2018. [Online]. Available: www.araconfiber.com/datasheets

[17] *Light Stitches Conductive Thread Datasheet*. Accessed: Jan. 2, 2018. [Online]. Available: http://www.lightstitches.co.uk/product/conductive-thread-reel-182m-approx

[18] *Alpha Wire 2840/7 PTFE Insulated Flexible Wire Datasheet*. Accessed: Jan. 2, 2018. [Online]. Available: www.alphawire.com/Home/Products/Wire/Hook-Up-Wire/Premium/2840_7

[19] *Specifications for Particular Types of Winding Wires. Solderable Polyurethane Enamelled Round Copper Wire, Class 155*, document BS EN 60317-20:2014, 2014.

[20] E. Heo, K.-Y. Choi, J. Kim, J.-H. Park, and H. Lee, "A wearable textile antenna for wireless power transfer by magnetic resonance," *Textile Res. J.*, pp. 1–9, Feb. 2017.

[21] *Texas Instruments bq51013AEVM-765 Evaluation Module User Guide*. Accessed: Jan. 2, 2018. [Online]. Available: www.ti.com/lit/ug/sluu911a/sluu911a.pdf

Neil J. Grabham received the M.Eng. (Merit) degree in information engineering and the Ph.D. degree from the University of Southampton, U.K., in 1998 and 2002, respectively.

He is currently a Senior Research Fellow with Electronics and Computer Science, University of Southampton. His current research covers smart fabrics, energy harvesting, sensor technology, and wireless sensor networks.

Yi Li received the B.Eng. degree in automation from Guangxi University, China, in 2010, and the Ph.D. degree from the University of Southampton in 2015. His Ph.D. thesis was on wireless power supply for ambient assisted living.

He is currently working in the area of wireless power supply technologies for ambient-assisted living systems.

Lindsay R. Clare received the B.Sc. degree in electrical and electronic engineering from Swansea University in 1987, and the Ph.D. degree in power conditioning for energy harvesting in 2010. Since 2003, he has been a Research Assistant at University of Bristol working on various energy-harvesting-related projects.

Bernard H. Stark received the M.S. degree in electrical engineering from the Swiss Federal Institute of Technology (ETH), Zürich, in 1995, and the Ph.D. degree in engineering from Cambridge University, U.K., in 2000.

He is currently a Reader in Electrical and Electronic Engineering with the University of Bristol, and a member of the Electrical Energy Management Research Group. His research interests include renewable power sources and power electronics.

Stephen P. Beeby (M'03–SM'11) received the B.Eng. (Hons.) degree in mechanical engineering from the University of Portsmouth, U.K., in 1992, and the Ph.D. degree from the University of Southampton, U.K., in 1998.

He is currently the Head of the Smart Electronic Materials and Systems Research Group, University of Southampton. His research interests include energy harvesting, e-textiles, MEMS, and active printed materials development.